Smart Materials and Structures

PAPER • OPEN ACCESS

Fully 3D printed soft microactuators for soft microrobotics

OPEN ACCESS
IOP Publishing

Smart Materials and Structures

Smart Mater. Struct. **29** (2020) 085032 (11pp)

https://doi.org/10.1088/1361-665X/ab9f48

Fully 3D printed soft microactuators for soft microrobotics

Manav Tyagi[1,2], Geoffrey M Spinks[2] and Edwin W H Jager[1,2]

[1] Sensor and Actuator Systems, Department of Physics, Chemistry and Biology (IFM), Linköping University, Linköping 58183, Sweden
[2] Australian Institute for Innovative Materials, University of Wollongong, Wollongong NSW 2522, Australia

E-mail: edwin.jager@liu.se

Received 11 March 2020, revised 19 May 2020
Accepted for publication 23 June 2020
Published 10 July 2020

Abstract

The feasibility of additive manufacturing actuating microstructures and microdevices with small dimension is presented. Using a custom-built extrusion 3D printer and CAD model of the device structure, bilayer microactuators driven by hydrogels are fabricated down to a size of $300 \times 1000\ \mu m^{2,}$ with a minimum thickness of 30 μm. To explore the limitations of the 3D printing process, microactuators with a width of 300 μm and lengths ranging from 1000 to 5000 μm are manufactured and thereafter operated to demonstrate the feasibility of the process. Similarly, microrobotic devices consisting of a passive rigid body and flexible moving parts are 3D printed to illustrate the ease and versatility of the additive manufacturing technique to fabricate soft microgrippers or micromanipulators.

Supplementary material for this article is available online

Keywords: 3D printing, hydrogel, microactuators, microrobotics, soft robotics

(Some figures may appear in colour only in the online journal)

1. Introduction

Constructed from compliant materials, soft robots have greater flexibility to adapt to unstructured environments and perform complex functions that are difficult to achieve using conventionally built rigid robots [1]. The enhanced versatility and compliancy of the soft actuators allow them to safely interact in close proximity or even in contact with humans. Soft matter requires manipulation with soft actuators that tend to be non-harmful or non-invasive. Soft robots, due to the enhanced flexibility, have better reach in constrained spaces than the rigid ones. Likewise, soft microrobotics allows for the grasping and manipulation of small delicate objects with potential applications in the fields of medical technology and space. Therefore, soft microrobots are interesting candidates for minimal invasive surgery, endoscopy and drug delivery [2]. Soft robots can also be deployed in space to attach to surfaces by changing shapes and move robustly against the gravity like a caterpillar [3]. Design and fabrication of these soft microrobots and soft microactuators, is therefore, of utmost importance to develop the field of microrobotics and to extend its applications in various domains.

Soft robotic actuators, at the micro-scale, are conventionally manufactured using the microfabrication techniques, such as photolithography [4–6], soft lithography [7, 8], and laser ablation [7, 9]. Lately, soft actuators on the macro-scale have been increasingly fabricated using the additive manufacturing techniques, mainly 3D printing [10–13]. Additive manufacturing techniques not only provide an easier fabrication workflow from design to product, but can also potentially reduce waste production since the materials are added layer by layer (on-demand) to create a desired structure [14]. Prototyping with 3D printing is fairly swift, with a simpler design to product process, enabling easier and more rapid product development.

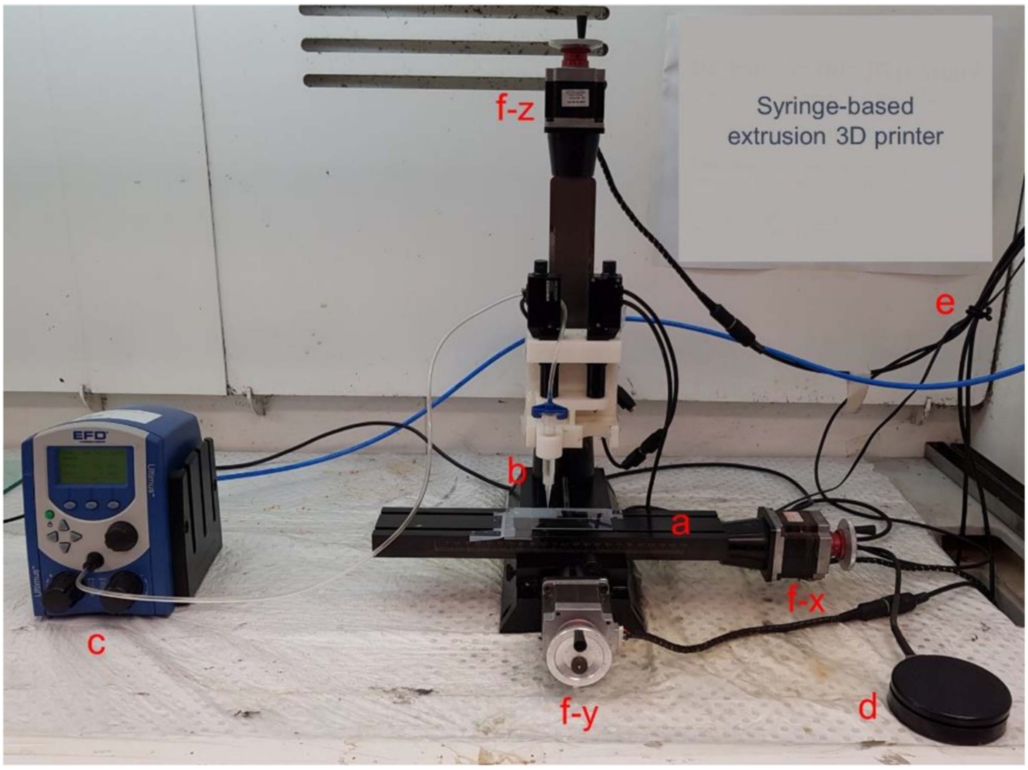

Figure 1. Photograph of the custom-built extrusion 3D printer showing the individual parts: (A) printing stage; (B) dispense syringe; (C) fluid dispenser; (D) dispenser control; (E) cables to computer; and (F) motors controlling the stage in x, y, z direction.

Fabrication of soft actuators via additive manufacturing, therefore, is interesting and has been reported in the literature, however only on the macro-scale. Soft actuators have been 3D printed to achieve variety of applications and the process is sometimes referred to '4D printing' [15, 16]. Recently, Scharff *et al* utilized 3D printing to fabricate soft actuators with integrated colour based proprioceptors to sense the interaction of the soft actuators with unstructured environment [17]. Soft actuators driven by shape memory alloys were 3D printed using inkjet printing of multiple soft materials, allowing them to exhibit various bending motions [18]. Similarly, fast-responsive soft actuators with tunable mechanical properties were fabricated utilizing a commercially available multimaterial 3D printer [19]. Truby *et al* fabricated soft robotic fingers with tactile feedback using 3D printing to function as flexible grippers with multiple degrees-of-freedom [20]. Sundaram *et al* using multimaterial drop-on-demand printing, fabricated magnetic actuators with soft and rigid polymers to achieve complex, integrated functionalities [21].

Soft robotics is extending its application in the micrometre domain, however current 3D printing of soft actuators is limited to the millimetre scale and above. To advance miniaturization of soft robots, additive manufacturing techniques need to be developed to fabricate microrobotic structures and devices. As a proof-of-concept and to explore the limitations of 3D printing soft microactuators, we are demonstrating the feasibility to fabricate bilayer microactuators at the micro-scale using extrusion 3D printing. In this study we push the limits of 3D printing to test how small microactuators can be fabricated exclusively with 3D printing. We have previously shown that additive manufacturing of soft microactuators and microrobots can be pushed into the microdomain using a hybrid additive manufacturing approach [22]. Instead of microfabricating the complete structure via 3D printing, we used a hybrid method that combined 3D printing with conventional polymer synthesis to fabricate the entire microactuator device. We used 3D printing only to fabricate the passive structural elements of the device on a conductive substrate prepared with sputter deposition. As for the active material, we used electrosynthesis of electroactive polymers to fabricate a layer of polypyrrole on the passive structure to drive the actuators. This previous work showed that we could fabricate microrobots with various designs and dimensions down to 300 μm wide and 20 μm thick with a 3D printer, but it did utilize other classical methods to manufacture the entire microactuator. These are the smallest microactuators thus far produced using a 3D printing process.

In the present work we explored the possibilities of completely 3D printing the microrobot in a simple, continuous procedure and investigated the size limitations of the chosen method. Instead of using a hybrid approach to fabricate the microactuator [22], we fabricated the entire device structure exclusively using 3D printing. We fabricated both the passive structural parts of the microactuator and the active driving material in a single process with an extrusion 3D printer. Conducting polymers, especially polypyrrole, are interesting driving materials for soft microrobotics [23]. Cullen *et al* have recently demonstrated 3D printing of polypyrrole using a special UV curable formulation for the first time,

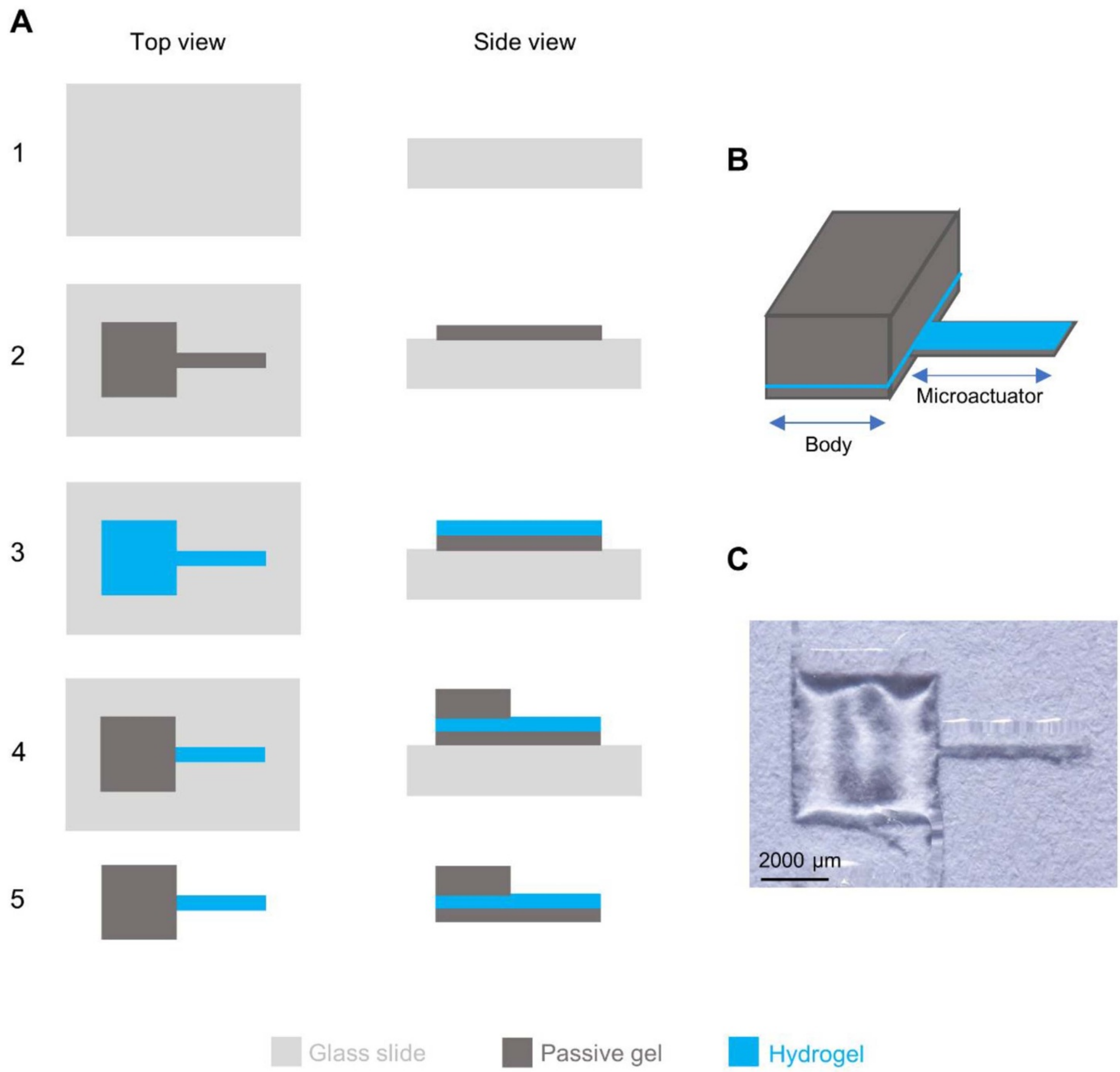

Figure 2. (A) Schematic diagram illustrating the fabrication steps: (1) clean glass slide; (2) extrusion print passive gel layer to form the structural layer; (3) print the active hydrogel layer over the structural layer; (4) print successive passive gel layers to form rigid body; and (5) remove the printed microrobot by peeling-off. (B) 3D sketch of microrobot showing the printed bilayer passive body and microactuator. (C) Photograph of the fabricated bilayer microrobot with body before removing from the glass slide.

however electromechanical actuation was not demonstrated [24]. Therefore, to demonstrate the feasibility in this conceptual work, we use hydrogels as the driving material. Hydrogels have readily available formulations that can be printed and actuated at the macro-scale [15, 25]. Hydrogels are hydrophilic polymer gels that can undergo expansion with exposure to moisture, exhibiting large volume changes or deformations [26, 27]. They are particularly interesting in fabricating compliant soft actuators because of high water content, flexibility, biocompatibility and adaptability to various stimulus and environments [28–30]. Water being non-toxic and easily available in variety of environments, is an interesting candidate to actuate the soft microactuators. Using hydration as the source to drive motion could have advantages in designing soft actuators where water acts as the trigger, e.g. automated valves to control the flow of water. Hydrogels have been 3D printed to fabricate soft actuators and robots with various applications such as microfluidic valves [15, 31], for tissue engineering [32–34], and printing organs for medical applications [35, 36].

As a proof of concept of fully 3D printing soft microactuators, we fabricated the entire microrobot i.e. the hydrogel-based microactuators combining the active and passive body using a custom-built extrusion 3D printer. We take our hybrid printed microrobot as the starting point [22], and take inspiration from the work of Naficy *et al* of using shape morphing hydrogels as the actuating material [25]. They studied a series of 4D printed hydrogels to fabricate actuating structures using an extrusion printer and developed a simple model to predict the bending characteristics of shape morphing actuators. They fabricated

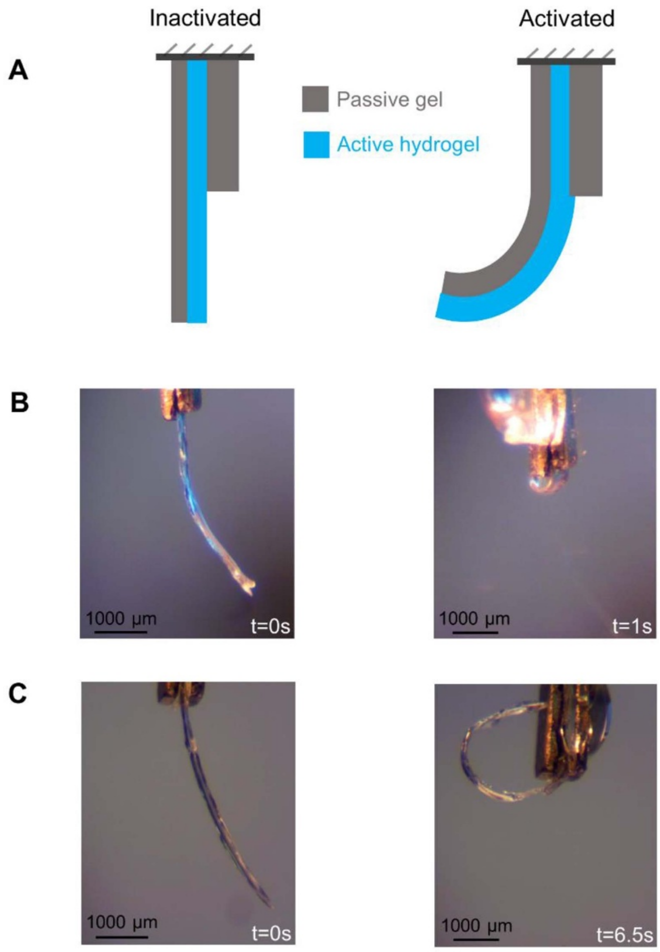

Figure 3. (A) Schematic diagram illustrating the actuation motion on hydration. (B) Very fast sub-second actuation of the microactuator when dipped in water, the actuation motion was too fast to capture due to camera's limited framerate. The left image shows the microactuator before water immersion and the right image shows the immersed microactuator as completely bent and stuck to the metal pin. (C) Fast actuation of the microactuator when sprayed with water, the actuation motion was slower due to slower water intake. The left image shows the microactuator before spraying and the right after spraying with water.

soft actuators using 3D printing, but demonstrated the actuating structures only up to the millimetre scale, in the range of 10–20 mm with thickness of 1.75 mm. They 3D printed bilayer structures composed of two different active hydrogel materials that could change shape on exposure to water. The disproportional swelling of the two different hydrogels in each layer generated the bending motion.

In the present work, we demonstrate fully printed soft microactuators and microrobots and investigate the dimensional limits of fabricating these devices. We study the feasibility of fabricating microactuators at the micro-scale in a single process with an extrusion 3D printer. Also, we demonstrate 3D printing of two different materials to integrate active and passive layers within an actuator device. In contrast to using two active hydrogel materials to drive the bending mechanism [25], we 3D print two completely different materials: one passive gel to provide the structural integrity and one active gel to provide the actuation of the microactuator. Combining a passive and active material in a single device structure results in better control over the bending motion by inducing actuation in only one layer. The passive material governs the rigidity or flexibility of the microactuator, whereas the active layer governs the bending motion just using hydration/dehydration.

2. Materials and methods

2.1. Materials

Ebecryl 4491, a UV curable aliphatic urethane acrylate gel, was purchased from Allnex Belgium and used as received. It was used as the passive gel material for providing structural integrity to the microactuators. Commercially available hydrogel, Hydromed D4, was purchased from AdvanSource Biomaterials (USA). The printing ink was prepared by dissolving the Hydromed D4 in ethanol (with 1 wt% water) to a concentration of 20%. It was used as the active gel material providing the actuation motion. Standard microscopic glass slides were cleaned with ethanol and isopropyl alcohol, dried with nitrogen gas, and used as the substrate for 3D printing.

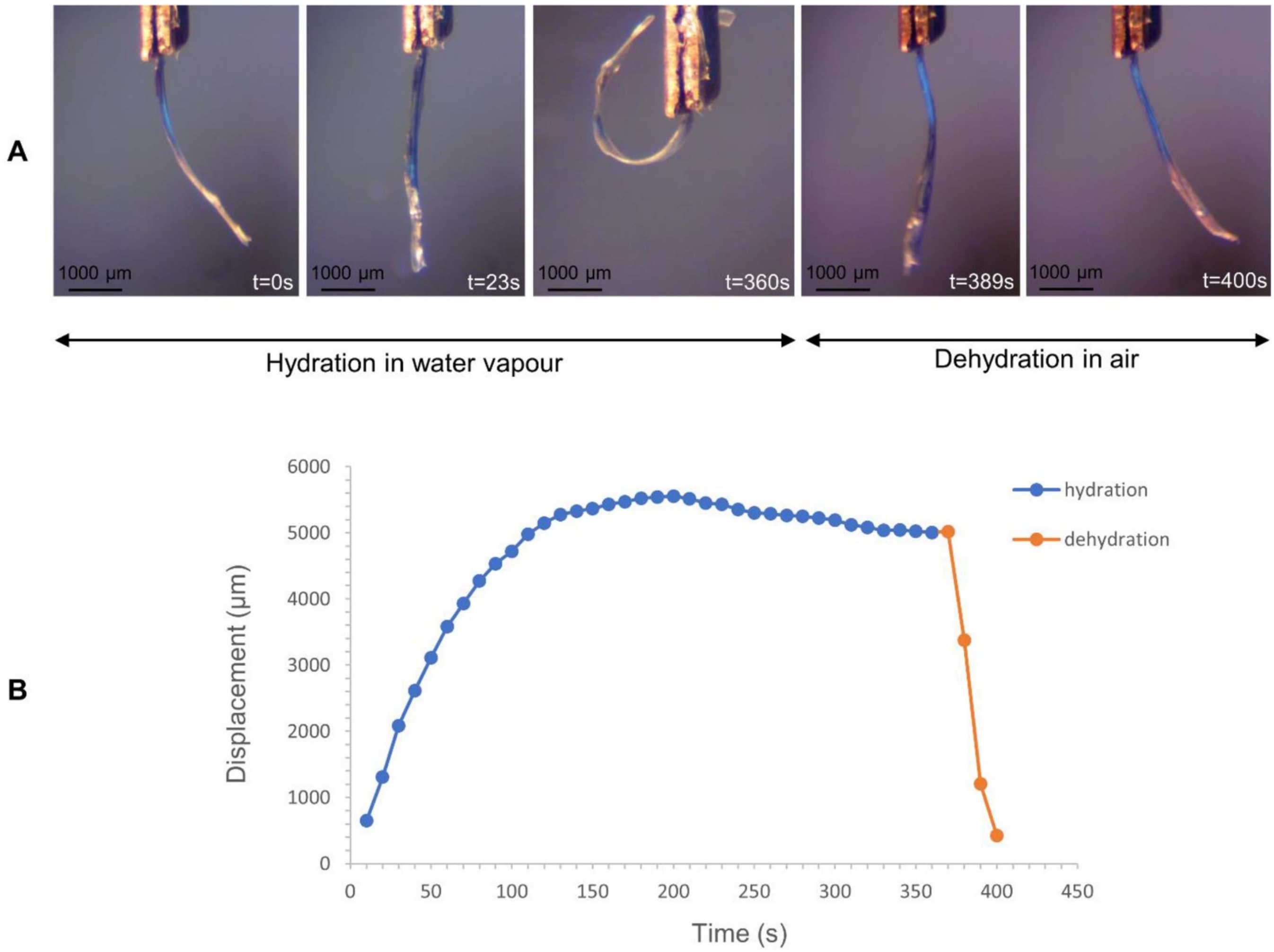

Figure 4. (A) Motion of the bilayer hydrogel microactuator during actuation (hydration) with water vapour and deactuation (dehydration) in air at ambient conditions. Actuation with water vapour slows the hydration rate of hydrogels resulting in a slower, controlled movement for characterization. (B) Graph showing the relation between the time of hydration/dehydration versus the tip displacement for the bilayer microactuator. The reduction in tip displacement after 200 s during hydration is due to the bending of the microactuator more than 180 degrees, bringing the final position of the microactuator tip closer to the initial starting point. See supplementary information for video animation.

2.2. 3D printer design

For 3D printing microactuators we used a custom-built, syringe-based extrusion 3D printer [37], consisting of a 3-axis (x, y, z) programmable CNC milling stage (Sherline 8020) and a high-precision fluid dispensing system (Ultimus, Nordson EFD) (figure 1). A Luer lock syringe (5 ml) fitted with tapered tip (Gauge 27, ID 0.20 mm, Nordson EFD) was used to dispense gel. The resolution of an extrusion 3D printer depends on several factors such as the dimensions of the extrusion tip, flow properties of the ink gel material, extrusion rate and the movement of stage motors. The resolution of the stage motors used in the custom-built 3D printer is 25 μm which sets a lower limit on the x-y resolution. The z resolution is smaller because evaporation of solvent reduces the printed layer thickness. We optimized the parameters for the chosen extrusion tip and ink gel used, considering the quality of print line. We observed if the printing had breaks in the line or if the ink gel was overflowing, and considering these, we decided on the following parameters. The rate of extrusion (printing) was controlled by the lateral motion of the stage (~ 2.5 mm s^{-1}) along with the dispensing air pressure (50–65 psi).

2.3. Device design

The process of 3D printing starts with a CAD model or software design of the structure or device that needs to be printed. We programmed the design directly in G-code using Linux-CNC/AXIS software (version 2.5.0) to design the structure of the microactuators. The G-code directly instructed the 3D printer to move along the 3 directions (x, y, z axis) with intended position and speed.

2.4. 3D printing soft microrobot

We started with a clean microscopic glass slide to print the structures. A single layer of Ebecryl 4491 (passive gel) was printed using the extrusion 3D printer to form the body and microactuator of the microrobot. For a thicker passive layer,

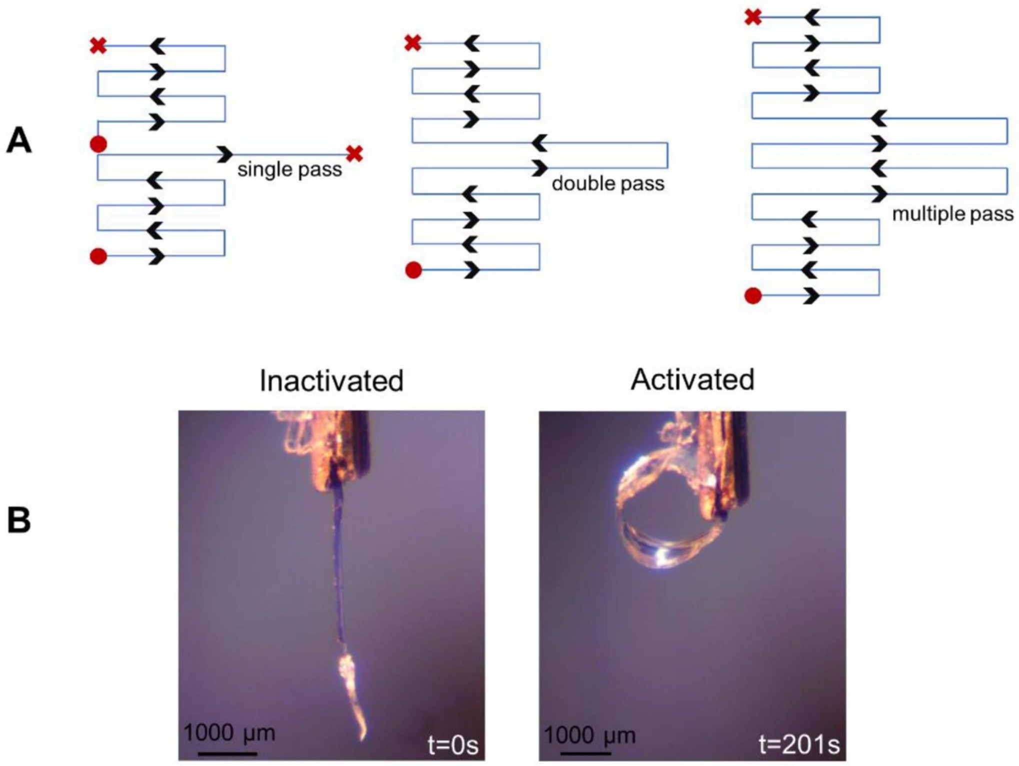

Figure 5. (A) Figure depicting the direction of movement of the extrusion tip to print the microactuator structure with extrusion 3D printer. The red circular sign shows the starting point and the red cross sign the termination point. The black arrows show the direction of extrusion printing. (B) Actuation of the microactuator 3D printed with just double pass of the printer, resulting in a narrow microactuator of width 300 μm (table 1).

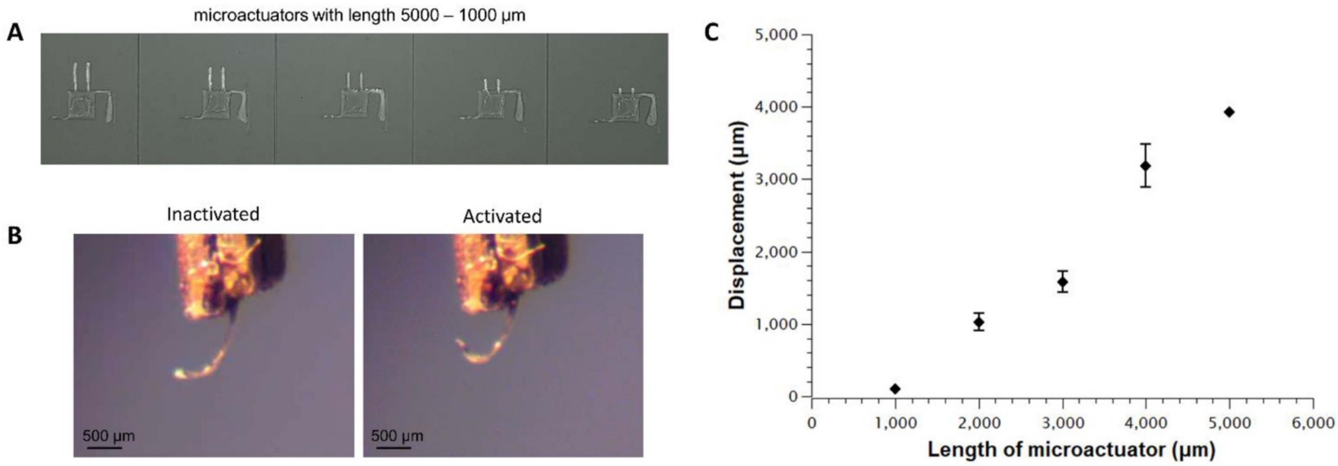

Figure 6. (A) Microactuators with varying lengths. (B) Actuation of the smallest microactuator. (C) Microactuator displacement for the actuators prepared with different lengths and exposed to water vapours for 60 s.

we printed two layers of the passive gel in succession. Thereafter, the printed structure was cured with a UV light source (280–450 nm, 19 W cm^{-2}) for 60 s (Dymax BlueWave 75). Then, we 3D printed one or two layers of active hydrogel layer over the passive structure and kept it at room temperature for 1 h to let the solvent evaporate, setting the hydrogel structure. For printing the second layer of hydrogel, we did not account for the change in size laterally due to solvent evaporation. However, for a successive deposition of the hydrogel layer on top, we manually adjusted the height of the extrusion syringe tip at an optimum distance for printing the next layer. Subsequently, we printed additional layers of passive gel over the body part and cured it with UV light to enhance rigidity of the microrobot, allowing for motion only in the flexible microactuator. We fabricated several samples with identical parameters (~5) to do the characterization studies. The 3D printing steps involved with the fabrication of hydrogel based microrobot are shown in figure 2.

Table 1. Table listing the width of microactuators 3D printed with various passes (lines) of the extrusion tip.

Pass (line)	Width of the microactuator (μm)
Single	200
Double	300
Multiple	1000

2.5. Actuation

Hydrogel based bilayer actuators swell or actuate with water, either in the liquid or vapour form. To achieve this volume change in a controlled fashion, we devised a simple set-up for characterization. We used a glass beaker quarter-filled with DI water and kept it over a hot plate at 50 °C for 20 min, to form vapours at a slow steady rate. Then, the microactuator is fixed upside down on a flat glass plate with attached metal clips and placed over the glass beaker such that the actuator lies in the empty volume receiving the water vapour. In this conceptual study, we obtained microactuator motion just using a steady source of water vapour. To keep the bending constant for all samples, we did not alter the humidity levels for our microactuator devices. To record the motion of the microactuator, we used a portable USB microscope (ToupTek, Optek). To match the monofocal lens of the microscope, the distance between the microscope and actuator was carefully adjusted to try to keep the entire actuator in focus during motion. To ensure enough exposure for brighter images, an external lamp was used.

3. Results and discussion

3.1. Fabrication of microactuators

Initially, we wanted to check the feasibility of our fabrication process and to see if the 3D printed hydrogel microactuators actuated when exposed to moisture. For this initial evaluation, we 3D printed a hydrogel bilayer microactuator that was 1000 μm wide, 4000 μm long and 65 μm thick, attached to the rigid body that was 3000 μm wide, 5000 μm long and 450 μm thick. To actuate the device, we dipped the microactuator in water and noticed a very fast bending response (figure 3(B)). The thin hydrogel layer swelled almost instantaneously, too fast to capture properly due to the camera's limited frame rate. We tried slowing the water uptake of the hydrogel by spraying the microactuator with a water mist, but this process also resulted in a fast actuation (figure 3(C)).

To capture the full motion properly we therefore chose to activate our 3D printed microactuators using a slow and steady source of water vapour (figure 4). We fabricated 5 samples with identical parameters that all showed similar behaviour of the actuation motion. Figure 4(A) shows the actuation motion of such a typical 3D printed microactuator sample. The exposure to the vapour ensured a slower swelling than direct water immersion and gave a limited (and observable) rate of bending, as described in section 2.5. This method allows for the measurement of accurate actuation levels, achieving intermediate bending positions depending on the time the actuator is subjected to hydration (figure 4(B)). As can be seen in figure 4, the microactuator actuated as expected when subjected to water vapour, requiring 360 s to bend completely from the inactivated (dehydrated) state. The final position of the microactuator was limited by the metal clip holding it, and if allowed to touch the metal clip, the tip of the microactuator would sometimes stick making it harder (longer) to release and come back to the neutral position. When sticking was avoided, the microactuator was observed to return to its original dehydrated (inactivated) position much faster than the activation (figure 4(B)). The dehydration step was simply in air at ambient conditions without the water source. These hydrogel-based microactuators could be reactivated/deactivated for multiple cycles. The in-depth performance and lifetime characterizations were out of the scope of this paper, and therefore, we plan to pursue these studies in future work.

3.2. Micro 3D printing

Having shown the complete 3D printing of the hydrogel based microactuators and its successful actuation, we fabricated microactuators with various dimensions to explore the limitations of the fabrication process. We 3D printed microactuators with similar length and thickness, but narrower than 1000 μm to investigate how narrow we can fabricate the microactuators. To reduce the microactuator width, we 3D printed microactuators just using a double pass (two lines) of the 3D printer (instead of multiple pass) to form the actuator [22]. In this process the printer deposited the gel in a continuous U-shaped fashion instead of just terminating at the tip of the microactuator (figure 5(A)). Although we could have scaled down further the width of the microactuators with just a single pass of the printer (one line), we determined that better quality structures were achieved by continuous printing (table 1). Due to the viscous nature of gel, it was observed that terminating the printing process (gel extrusion) at the microactuator tip would often result in the deposition of an unwanted drop of gel, which would then require additional cutting afterwards to finalize the desired shape. Figure 5(B) shows the actuation of the narrowest microactuator fabricated with double pass, that was 300 μm wide, 3000 μm long and 45 μm thick, whereas the rigid body was 5000 μm wide, 5000 μm long and 400 μm thick.

Thereafter, we fabricated microactuators with arm lengths ranging from 5000 down to 1000 μm, with same width and thickness (300 μm and 45 μm respectively), and the rigid body was 2500 μm wide, 5000 μm long and 400 μm thick (figure 6(A)). We then actuated these actuators with water vapour to examine the bending motion. As expected, the microactuators with longer lengths showed larger tip displacements in a given time of actuation (figure 6(C)), in agreement with the bending beam theory [38, 39]. Several samples were made with 2000 μm, 3000 μm and 4000 μm length and the actuation displacement was found to be highly repeatable with less than 10% standard deviation.

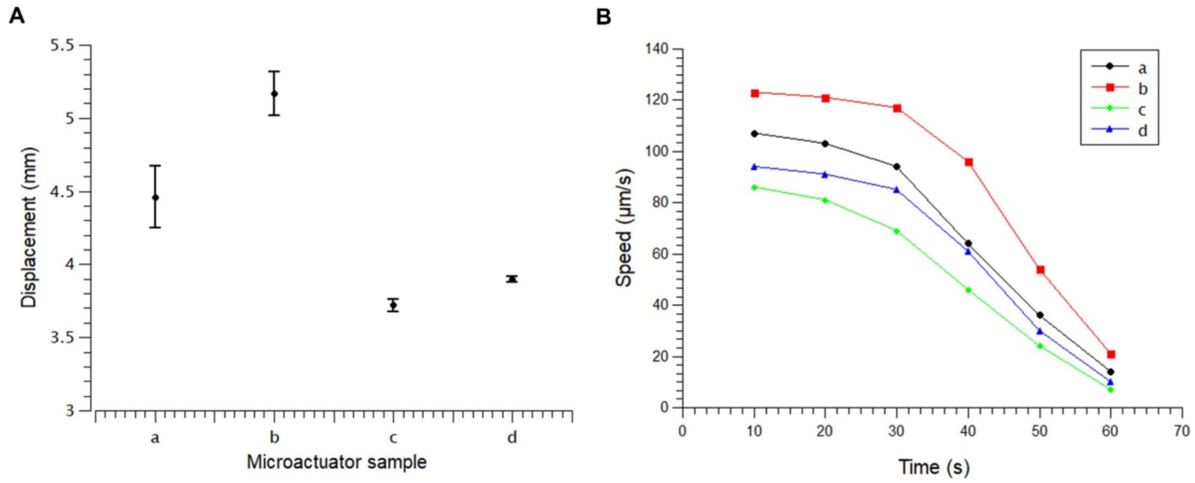

Figure 7. (A) Graph showing the displacement for 3D printed microactuator samples with varying thickness of active and passive layers after 60 s of actuation under hydration with water vapour. (B) Graph showing the variation in speed of actuation motion for 3D printed microactuator samples during hydration for 60 s, measured at an interval of 10 s.

Table 2. Table showing the microactuator samples 3D printed with varying thickness of active and passive layers to study the dependence of bending motion on layer thickness of microactuator.

Microactuator sample	Number of passive gel layers	Number of active gel layers	Total thickness of microactuator (μm)
a	1	1	30
b	1	2	45
c	2	1	54
d	2	2	71

3.3. *Effect of layer thickness on bending motion*

To study the effect of thickness of gel layers (active and passive) on the bending motion of the microactuator, we 3D printed microactuators in different combination of printed layers. We 3D printed four kinds of microactuators with similar dimension, but with variation of 1–2 layers for each active and passive gels as presented in table 2. The 3D printed microactuators were 300 μm wide and 5000 μm long, whereas the rigid body was 3000 μm wide, 5000 μm long and 400 μm thick. We observed that 3D printing successive layers of the active hydrogel on top of each other was difficult since the hydrogel used has low viscosity resulting in overflow of the layer. Also, the hydrogel layer shrinks after printing due to the evaporation of alcohol solvent, resulting in a decrease of the total thickness of the layer after printing. These shape and dimensional changes complicate the process of depositing successive layers even more since the height alteration required for the gel extrusion tip to print over the top layer had to be adjusted manually in our custom-built 3D printer. Therefore, we decided to print only a maximum of two hydrogel layers for the microactuator characterization. We also decided to print only a maximum of two layers for the passive gel. Although extrusion printing of additional layers of the passive gel is comparably easier (as for the body), we chose to keep the symmetry of the microactuating device structure for the sake of simplicity.

The tip displacement of all four microactuators was determined after 60 s exposure to the hydrating environment (figure 7(A)). As observed, the tip displacement varied by almost a factor of 1.5 with the largest displacement occurring in the microactuator fabricated with two active layers and one passive layer (sample b). Tip displacement in bilayers involves a complex interaction between the layer thicknesses, the ratio of the layer elastic moduli and the difference in swelling strain of the two layers [25]. The tip displacement generally increases with an increasing ratio of the active layer thickness to the passive layer thickness. Swelling of the active layer generates the torque needed to bend the bilayer and a larger torque is expected with thicker active layers providing faster speed of motion (figure 7(B)). In addition, the speed of actuation motion is enhanced when the stiffness of the bilayer decreases and the bending stiffness in our system is dominated by the passive layer because of the considerably higher modulus of the passive layer material in comparison with the hydrated hydrogel [8, 38]. These considerations explain why the displacement and the speed of the microactuators increased with an increasing ratio of active layer to passive layer thickness, and vice versa (sample c). It is also noted that a faster actuation and larger tip displacement was observed in the microactuator prepared with 1 active layer and 1 passive layer (sample a) in comparison with the microactuator fabricated with 2 active and 2 passive layers (sample d). The diffusion of water into the active layer controls the rate of actuation, and it is likely that a higher degree of water penetration occurred in the microactuator with only one active layer compared with that made with 2 active layers.

3.4. *3D printing microrobots*

To explore the versatility of the developed 3D printing process, we printed microrobots with varying structure and dimensions. To control the bending motion in these devices, we printed active and passive regions within the structures using active hydrogel and passive UV curable gel. We 3D printed two

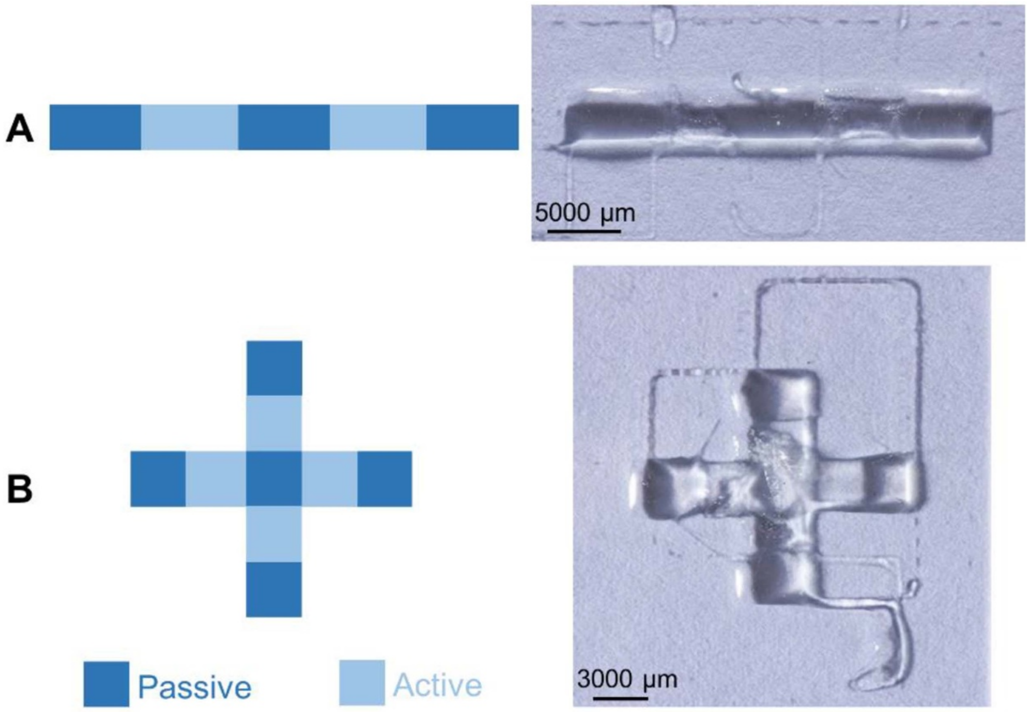

Figure 8. (A) Graphical sketch and actual photograph of the fabricated microrobot with two flexible microactuators, comprising of active and passive sections each of the dimension $3000 \times 5000\ \mu m^2$. (B) Graphical sketch and actual photograph of the fabricated microrobot with four flexible microactuators, comprising of active and passive sections each of the dimension $3000 \times 3000\ \mu m^2$.

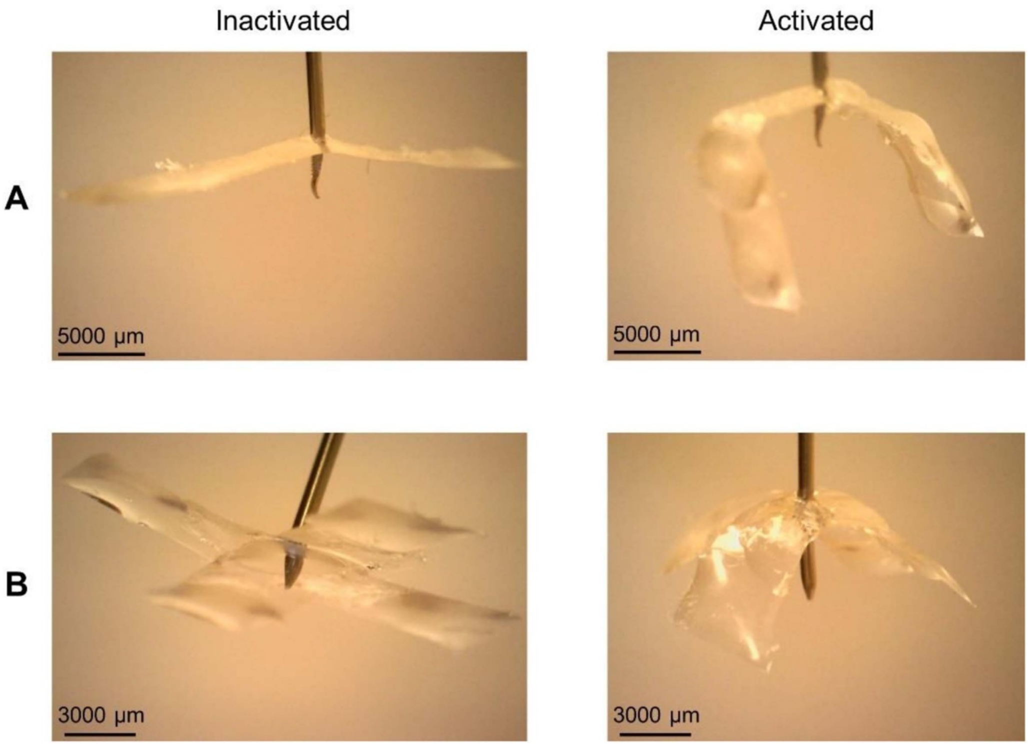

Figure 9. (A) Actuation of the microrobot with two flexible microactuators. The image on the left shows the microrobot before actuation and the image on the right after actuation, showing the two microactuators bending. (B) Actuation of the microrobot with four flexible microactuators. The image on the left shows the microrobot before actuation and the image on the right after actuation, showing the four microactuators bending. See supplementary information for video animations.

kinds of microrobots, a linear snake-like microrobot with two microactuators and a microgripper-like with four microactuators (figure 8). The two active (microactuator) and the three passive (body) sections of the snake-like microrobot were $3000 \times 5000\ \mu m^2$ each (figure 8(A)). The microgripper-like microrobot consisted off four active and five passive sections of $3000 \times 3000\ \mu m^2$ each (figure 8(B)). These microrobots were thereafter actuated to observe the bending motion (figure 9). The microactuators in these microrobots activated on hydration, allowing for the bending motion only in the active sections behaving as hinges. The scalability and movement of these soft microrobotic devices can be adjusted by modifying dimensions of the active and passive layers while 3D printing to obtain microrobots with desired functionality. Material properties also play an important role in determining the bending characteristics. For instance, utilizing a more flexible passive material or a more hygroscopic active gel in these microrobots would also result in a greater bending motion during actuation.

4. Conclusions

We successfully 3D printed the entire microactuator device using extrusion 3D printing and pushed the fabrication of microrobots in the micrometre domain. We developed a micro 3D printing process to miniaturize soft robotic bilayer actuators, in this example based on hydrogels, and fabricated smallest microactuator with dimension of $300 \times 1000\ \mu m^2$ and thickness 30 μm, thus demonstrating the scalability.

The fabricated microactuators were highly responsive in the presence of water, with very fast actuation speeds, especially when submerged in water. The displacement or bending of these 3D printed microactuators could be slowed down by adjusting the actuation medium (water vapour), allowing for more accurate actuation levels for desired bending movement or angle. Furthermore, we successfully 3D printed active and passive layers in a single microactuator structure. We presented the 3D printing of two different materials in a single process to fabricate bilayer microactuator structures with a defined bending motion. To demonstrate the effect of individual materials, we fabricated and characterized microactuators with multiple layers of active and passive gels to study the impact on bending.

To illustrate the versatility of the developed 3D printing process, we fully printed microrobots with varied structures and dimensions and multiple active segments (hinges). It demonstrates that fabricating soft microactuators using extrusion 3D printing provides an easy and straightforward, yet powerful manufacturing process. This enables the fabrication of complex soft microrobots completely via 3D printing.

In this feasibility study we successfully demonstrated that the entire microactuator could be fabricated exclusively using 3D printing. In addition, we we could scale down the soft actuators to the micro dimensions using a simple, custom-built extrusion 3D printer. The actuation motion of the microactuator depends on the material properties and to enhance the performance of miniaturized microrobots, full characterisation the printable gels and their behaviour during actuation would be needed. Similarly, developing printing materials and methods for other means of actuation is also very interesting because it would pave the way for 3D printing a plethora of different kinds of microactuators and microrobots. In future work, for instance, we plan to replace the active hydrogels with electroactive materials such as polypyrrole to fabricate microactuators controlled by electrical stimulus [24]. We believe that with this proof-of-concept study to fabricate soft microactuators with 3D printing, the manufacturing of complex microrobots completely via 3D printing will become one step simpler and closer to reality.

Acknowledgments

We thank the EU Marie Sklodowska-Curie Actions Initial Training Network MICACT (641822), the Swedish Research Council (2014-3079) and the University of Wollongong's Visiting International Scholar Award and Global Challenges Program for their financial support.

Conflict of interests

The authors Manav Tyagi, Geoffrey M. Spinks and Edwin W. H. Jager declare no conflict of interest.

Contributions

Manav Tyagi, Geoffrey M. Spinks and Edwin W. H. Jager designed the experiments. Manav Tyagi performed the experiments. Manav Tyagi, Geoffrey M. Spinks and Edwin W. H. Jager wrote the manuscript.

ORCID iDs

Manav Tyagi https://orcid.org/0000-0002-7613-5003
Geoffrey M Spinks https://orcid.org/0000-0003-4656-9473
Edwin W H Jager https://orcid.org/0000-0002-2071-7768

References

[1] Rus D and Tolley M T 2015 Design, fabrication and control of soft robots *Nature* **521** 467
[2] Runciman M, Darzi A and Mylonas G P 2019 Soft robotics in minimally invasive surgery *Soft Robot.* **6** 423–43
[3] Trimmer B, Lin H-T and Leisk 2013 Soft robots in space: a perspective for soft robotics *Acta Futur.* **6** 69–79
[4] Jager E W H, Inganäs O and Lundström I 2000 Microrobots for micrometer-size objects in aqueous media: potential tools for single-cell manipulation *Science* **288** 2335
[5] Tasoglu S, Diller E, Guven S, Sitti M and Demirci U 2014 Untethered micro-robotic coding of three-dimensional material composition *Nat. Commun.* **5** 3124
[6] Medina-Sánchez M, Magdanz V, Guix M, Fomin V M and Schmidt O G 2018 Swimming microrobots: soft, reconfigurable, and smart *Adv. Funct. Mater.* **28** 1707228

[7] Ranzani T, Russo S, Bartlett N W, Wehner M and Wood R J 2018 Increasing the Dimensionality of Soft Microstructures through Injection-Induced Self-Folding *Adv. Mater.* **30** 1802739

[8] Tyagi M, Pan J and Jager E W H 2019 Novel fabrication of soft microactuators with morphological computing using soft lithography *Microsyst. Nanoeng.* **5** 44

[9] Sinatra N R, Ranzani T, Vlassak J J, Parker K K and Wood R J 2018 Nanofiber-reinforced soft fluidic micro-actuators *J. Micromech. Microeng.* **28** 84002

[10] Schaffner M, Faber J A, Pianegonda L, Rühs P A, Coulter F and Studart A R 2018 3D printing of robotic soft actuators with programmable bioinspired architectures *Nat. Commun.* **9** 878

[11] Haghiashtiani G, Habtour E, Park S-H, Gardea F and McAlpine M C 2018 3D printed electrically-driven soft actuators *Extrem. Mech. Lett.* **21** 1–8

[12] Zolfagharian A, Kouzani A Z, Khoo S Y, Moghadam A A A, Gibson I and Kaynak A 2016 Evolution of 3D printed soft actuators *Sensors Actuators* A **250** 258–72

[13] Yirmibesoglu O D, Morrow J, Walker S, Gosrich W, Cañizares R, Kim H, Daalkhaijav U, Fleming C, Branyan C and Menguc Y 2018 Direct 3D printing of silicone elastomer soft robots and their performance comparison with molded counterparts *2018 IEEE Int. Conf. on Soft Robotics (RoboSoft)* pp 295–302

[14] Paris H, Mokhtarian H, Coatanéa E, Museau M and Ituarte I F 2016 Comparative environmental impacts of additive and subtractive manufacturing technologies *CIRP Ann.* **65** 29–32

[15] Bakarich S E, Gorkin III R, Panhuis M I H and Spinks G M 2015 4D Printing with mechanically robust, thermally actuating hydrogels *Macromol. Rapid Commun.* **36** 1211–7

[16] López-Valdeolivas M, Liu D, D J B and Sánchez-Somolinos C 2018 4D printed actuators with soft-robotic functions *Macromol. Rapid Commun.* **39** 1700710

[17] Scharff R B N, Doornbusch R M, Doubrovski Z, Wu J, Geraedts J M P and Wang C C L 2019 Color-based proprioception of soft actuators interacting with objects *IEEE/ASME Trans. Mechatronics* **24** 1964–7

[18] Akbari S, Sakhaei A H, Panjwani S, Kowsari K, Serjouei A and Ge Q 2019 Multimaterial 3D printed soft actuators powered by shape memory alloy wires *Sensors Actuators* A **290** 177–89

[19] Zhang Y-F, Zhang N, Hingorani H, Ding N, Wang D, Yuan C, Zhang B, Gu G and Ge Q 2019 Fast-response, stiffness-tunable soft actuator by hybrid multimaterial 3D printing *Adv. Funct. Mater.* **29** 1806698

[20] Truby R L, Wehner M, Grosskopf A K, Vogt D M, Uzel S G M, Wood R J and Lewis J A 2018 Soft somatosensitive actuators via embedded 3D printing *Adv. Mater.* **30** 1706383

[21] Sundaram S, Skouras M, Kim D S, van den Heuvel L and Matusik W 2019 Topology optimization and 3D printing of multimaterial magnetic actuators and displays *Sci. Adv.* **5** eaaw1160

[22] Tyagi M, Spinks G M and Jager E W H 2020 3D printing microactuators for soft microrobots *Soft Robot.* accepted

[23] Jager E W H, Smela E and Inganäs O 2000 Microfabricating conjugated polymer actuators *Science* **290** 1540 LP–1545

[24] Cullen A T and Price A D 2019 Fabrication of 3D conjugated polymer structures via vat polymerization additive manufacturing *Smart Mater. Struct.* **28** 104007

[25] Naficy S, Gately R, Gorkin III R, Xin H and Spinks G M 2017 4D printing of reversible shape morphing hydrogel structures *Macromol. Mater. Eng.* **302** 1600212

[26] Peng X and Wang H 2018 Shape changing hydrogels and their applications as soft actuators *J. Polym. Sci.* B **56** 1314–24

[27] Yuk H, Lin S, Ma C, Takaffoli M, N X F and Zhao X 2017 Hydraulic hydrogel actuators and robots optically and sonically camouflaged in water *Nat. Commun.* **8** 14230

[28] Banerjee H, Suhail M and Ren H 2018 Hydrogel actuators and sensors for biomedical soft robots: brief overview with impending challenges *Biomimetics* **3**

[29] Zolfagharian A, A Z K, S Y K, Gibson I and Kaynak A 2016 3D printed hydrogel soft actuators *2016 IEEE Region 10 Conf. (TENCON)* pp 2272–7

[30] Rossiter J, Winfield J and Ieropoulos I 2016 Here today, gone tomorrow: biodegradable soft robots *Proc. SPIE* **9798** 97981S

[31] Ng W L, Lee J M, Yeong W Y and Win Naing M 2017 Microvalve-based bioprinting – process, bio-inks and applications *Biomater. Sci.* **5** 632–47

[32] Hockaday L A, Duan B, Kang K H and Butcher J T 2014 3D-printed hydrogel technologies for tissue-engineered heart valves *3D Print. Addit. Manuf.* **1** 122–36

[33] Derakhshanfar S, Mbeleck R, Xu K, Zhang X, Zhong W and Xing M 2018 3D bioprinting for biomedical devices and tissue engineering: a review of recent trends and advances *Bioact. Mater.* **3** 144–56

[34] You S, Li J, Zhu W, Yu C, Mei D and Chen S 2018 Nanoscale 3D printing of hydrogels for cellular tissue engineering *J. Mater. Chem.* B **6** 2187–97

[35] Yan Q, Dong H, Su J, Han J, Song B, Wei Q and Shi Y 2018 A review of 3D printing technology for medical applications *Engineering* **4** 729–42

[36] Schubert C, van Langeveld M C and Donoso L A 2014 Innovations in 3D printing: a 3D overview from optics to organs *Br. J. Ophthalmol.* **98** 159 LP–161

[37] Mire C A, Agrawal A, Wallace G G, Calvert P and Panhuis M I H 2011 Inkjet and extrusion printing of conducting poly(3,4-ethylenedioxythiophene) tracks on and embedded in biopolymer materials *J. Mater. Chem.* **21** 2671–8

[38] Pei Q and Inganaes O 1992 Electrochemical applications of the bending beam method. 1. Mass transport and volume changes in polypyrrole during redox *J. Phys. Chem.* **96** 10507–14

[39] Benslimane M, Gravesen P, West K, Skaarup S and Sommer-Larsen P 1999 Performance of polymer-based actuators: the three-layer model *Smart Structures and Materials 1999: Electroactive Polymer Actuators and Devices* vol 3669 (Int. Society for Optics and Photonics) pp 87–98